

Supporting Information

Contents

1. Synthesis of intermediate compounds.
2. X-ray crystal structure refinement parameters and special features
3. Spectroscopic, computational and electrochemical details.
 1. **Figures S1–S4.** Ambient temperature *Vs* 77 K, excitation spectra of complexes [9], [10], [11] and [13].
 2. **Table S1.** List of selected molecular orbital energies [eV] for the investigated complexes.
 3. **Table S2.** Isodensity surfaces plots of selected orbitals for the complexes [9], [10], [11] and [13].
 4. **Table S3.** Computed excitations energies and oscillator strengths for the complexes [9], [10], [11] and [13].
 5. **Figure S5.** Emission spectra of [9], [10], [11] and [13] in neat films.
 6. **Figure S6.** CV plots of complexes [9], [10], [11] and [13].
 7. **Figure S7.** NMR spectra of the ligand precursor (compound 7) and the NHC complexes [9], [10], [11] and [13].

Synthesis of intermediate compounds

Compound 2

To a solution of 1,1,1-trifluoro-2,4-pentanedione (12.95 g, 0.084 mol) in ethanol (110 mL) was added hydrazine hydrate (4.2 g, 0.084 mol) drop wise over 10 min. Reaction mixture was heated under reflux for 3 h and then cooled to 50 °C. Solvent was removed *in vacuo*. To the yellow syrup was added diethylether (40 mL) and the resulting solution washed with water. Organic phase was dried over MgSO₄ and diethylether was removed in rotary evaporator (800 mb, 40 °C). Upon cooling compound 2 was obtained as colorless to pale yellow solid. Yield: 9.9 g, (77 %). ¹H NMR (300 MHz, DMSO-*d*₆): δ 13.32 (s, 1H, N-H), 6.41 (s, 1H, C-H), 2.3 (s, 3H, methyl). ¹⁹F NMR (282 MHz, DMSO-*d*₆): δ -60.56. MS (ESI HRMS) *m/z* (%): 173.0297 (100) [2]⁺, (calcd. for [2]⁺ 173.0297).

Compound 3

An aqueous solution of KMnO₄ (3.8 g, 24 mmol in 35 mL of H₂O) was added dropwise into a solution of 2 (3.0 g, 20 mmol, in 55 mL of H₂O). The mixture was heated under reflux for 9 h. The reaction mixture was cooled to ambient temperature and the precipitated inorganic salts were filtered off over a bed of celite. The resultant filtrate was concentrated to 15 mL, followed by acidification using con. HCl. Resulting syrup or solid was suspended in diethylether and washed with H₂O. The ether phase was separated and dried over Na₂SO₄, and the solvents were removed *in vacuo*, to obtain compound 3 as colorless crystals. Yield: 1.85 g (51 %). ¹H NMR (300 MHz, DMSO-*d*₆): δ 14.74 (s, 1H, N-H), 7.24 (s, 1H, C-H), 5.78 (s, 1H, carboxylic -OH). ¹⁹F NMR (282 MHz, DMSO-*d*₆): δ -60.62. MS (ESI HRMS, Negative mode) *m/z* (%): 179.0075 (100) [3]⁺, (calcd. for [3]⁺ 179.0063).

Compound 4

1.6 mL of con. H₂SO₄ was added dropwise to a solution of 3 (1.75 g, 9.72 mmol) in absolute methanol (20 mL) and the resulting solution was stirred overnight at ambient temperature. Solvent was removed *in vacuo*, and the resultant residue was dissolved in water (15 mL) and transferred into a 250 mL round bottomed flask. The mixture was neutralized slowly using saturated NaHCO₃ solution to an alkaline pH (8), followed by extraction with ethyl acetate. The organic component was dried over Na₂SO₄, filtered and the solvent was removed *in vacuo*, to obtain crude sample of 4 as colorless solid, which was further purified on a silica gel column using hexanes/ethyl acetate (3:2) as eluent. Yield: 1.01 g (53 %). ¹H NMR (300 MHz, DMSO-*d*₆): δ 14.95 (s, 1H, N-H), 7.35 (s, 1H, C-H), 3.92 (s, 3H, -OCH₃). ¹⁹F NMR (282 MHz, DMSO-*d*₆): δ -60.63. MS (ESI HRMS) *m/z* (%): 217.0203 (100) [4+Na]⁺, (calcd. for [4+Na]⁺ 217.0201).

Compound 5

To a suspension of LiAlH₄ (587 mg, 15.6 mmol), in tetrahydrofuran (40 mL) in a two necked round bottomed flask was slowly added a solution of compound 4 (1.5 g, 7.7 mmol) in 20 mL of tetrahydrofuran. The resultant mixture was heated at 65 °C for 24 h, followed by slow quenching of the reaction with H₂O under rapid cooling. After evaporation of the solvents *in vacuo*, the reaction mixture was suspended in methanol (20 mL) and bubbled with CO₂ (gas) for 10 minutes, followed by heating under reflux for further 3 h. The reaction mixture was cooled and the solids were filtered off and methanol was removed *in vacuo*, to obtain pale yellow solids. The yellow solids were suspended in water and slightly acidified slightly followed by extraction using ethyl acetate (30 mL×3) and dried over Na₂SO₄. Solvents were removed *in vacuo*, to obtain compound 5 as colorless solid. Yield: 0.48 g (55 %). ¹H NMR (400 MHz, Acetone-*d*₆): δ 12.53 (s, 1H, N-H), 6.39 (s, 1H, C-H), 4.60 (s, 2H, -CH₂), 4.46 (t, *J* = 5.4 Hz, 1H, OH). ¹⁹F NMR (282 MHz, Acetone-*d*₆): δ -62.37. MS (ESI HRMS) *m/z* (%): 201.00441 (100) [5+Cl]⁺, (calcd. for [5+Cl]⁺ 201.0000).

Compound 6

To an ice cold solution of 5 (616 mg, 3.4 mmol) in diethylether (40 mL) was added a solution of PBr₃ (0.68 mL, 7.25 mmol) and stirred for 2 days, after which the reaction mixture was poured into 10 mL of cold water. The mixture was neutralized using saturated NaHCO₃ solution and the aqueous mixture was extracted with diethylether (20 mL×3) followed by dichloromethane (20 mL×3) sequentially. The combined organic layer was dried over anhydrous Na₂SO₄ and the solvent was removed *in vacuo*, to obtain compound 6 as colorless oil. Yield: 686 mg (88.23%). ¹H NMR (300 MHz, Acetone-*d*₆): δ 8.01 (s, 1H, NH), 6.74 (s, 1H, Ar-H), 4.72 (s, 2H, CH₂ bridge). ¹⁹F NMR (282 MHz, Acetone-*d*₆): δ -62.55. MS (ESI HRMS) *m/z* (%): 264.91811 (100) [6+Cl]⁺, 264.91704 (calcd. for [6+Cl]⁺).

X-ray crystal structure refinement parameters

X-ray crystal structure analysis of [9] (see CheckCIF file fro6223): formula $C_{24}H_{18}F_3N_5Pt$, $M = 628.52$, yellow crystal, $0.15 \times 0.15 \times 0.10$ mm, $a = 11.2790(2)$, $b = 17.2865(3)$, $c = 11.0836(2)$ Å, $\beta = 102.242(1)^\circ$, $V = 2111.88(6)$ Å³, $\rho_{\text{calc}} = 1.977$ gcm⁻³, $\mu = 6.694$ mm⁻¹, empirical absorption correction ($0.433 \leq T \leq 0.554$), $Z = 4$, monoclinic, space group $P2_1/c$ (No. 14), $\lambda = 0.71073$ Å, $T = 223(2)$ K, ω and ϕ scans, 10117 reflections collected ($\pm h, \pm k, \pm l$), $[(\sin\theta)/\lambda] = 0.67$ Å⁻¹, 3512 independent ($R_{\text{int}} = 0.051$) and 3251 observed reflections [$I > 2\sigma(I)$], 299 refined parameters, $R = 0.060$, $wR^2 = 0.161$, max. (min.) residual electron density $5.76(-3.08)$ e.Å⁻³, hydrogen atoms calculated and refined as riding atoms.

X-ray crystal structure analysis of [10] (see CheckCIF file fro6323): formula $C_{26}H_{16}F_9N_5Pt$, $M = 764.53$, yellow crystal, $0.33 \times 0.20 \times 0.20$ mm, $a = 10.3649(2)$, $b = 11.2201(3)$, $c = 11.8690(3)$ Å, $\alpha = 72.144(2)$, $\beta = 73.342(2)$, $\gamma = 77.339(1)^\circ$, $V = 1245.57(5)$ Å³, $\rho_{\text{calc}} = 2.038$ gcm⁻³, $\mu = 5.728$ mm⁻¹, empirical absorption correction ($0.253 \leq T \leq 0.394$), $Z = 2$, triclinic, space group $P\bar{1}$ (No. 2), $\lambda = 0.71073$ Å, $T = 223(2)$ K, ω and φ scans, 11385 reflections collected ($\pm h, \pm k, \pm l$), $[(\sin\theta)/\lambda] = 0.67$ Å⁻¹, 4266 independent ($R_{\text{int}} = 0.034$) and 4191 observed reflections [$I > 2\sigma(I)$], 399 refined parameters, $R = 0.020$, $wR^2 = 0.052$, max. (min.) residual electron density $0.85(-0.82)$ e.Å⁻³, hydrogen atoms calculated and refined as riding atoms.

X-ray crystal structure analysis of [11] (see CheckCIF file fro66517): formula $C_{26}H_{16}F_9N_5Pt$, $M = 764.53$, yellow crystal, $0.34 \times 0.30 \times 0.24$ mm, $a = 7.5972(1)$, $b = 22.2707(4)$, $c = 15.7810(4)$ Å, $\beta = 102.385(1)^\circ$, $V = 2607.93(9)$ Å³, $\rho_{\text{calc}} = 1.947$ gcm⁻³, $\mu = 5.471$ mm⁻¹, empirical absorption correction ($0.257 \leq T \leq 0.353$), $Z = 4$, monoclinic, space group $P2_1/c$ (No. 14), $\lambda = 0.71073$ Å, $T = 223(2)$ K, ω and φ scans, 23180 reflections collected ($\pm h, \pm k, \pm l$), $[(\sin\theta)/\lambda] = 0.66$ Å⁻¹, 4316 independent ($R_{\text{int}} = 0.039$) and 4071 observed reflections [$I > 2\sigma(I)$], 408 refined parameters, $R = 0.028$, $wR^2 = 0.072$, max. (min.) residual electron density $0.98(-1.17)$ e.Å⁻³, hydrogen atoms calculated and refined as riding atoms.

Exceptions and special features: Compound [9] contains one fluorine atom (F19) with irregular displacement ellipsoid, which was therefore constrained to be more regular using the program command ISOR. For the compound [10] a disordered over two position CF₃ group was found. Several restraints (SIMU, ISOR and SADI) were used in order to improve refinement stability. For the compound [11] one disordered CF₃ group over two positions was found. Several restraints (SADI, SAME, SIMU and ISOR) were used in order to improve refinement stability. The fluorine atoms from one CF₃ group displayed irregular displacement ellipsoids, which were therefore constrained to be more regular using the program command ISOR.

Spectroscopic, computational and electrochemical details.

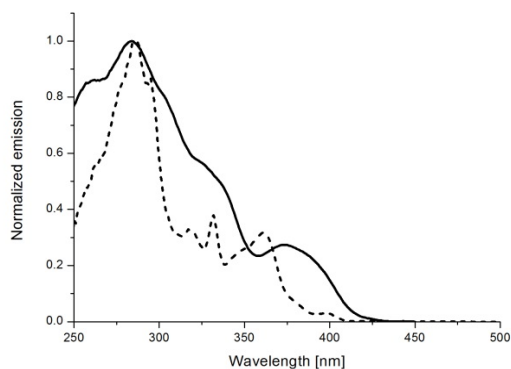


Figure S1. Excitation spectra of complex [9] at rt (solid line) and 77 K (dashed line).

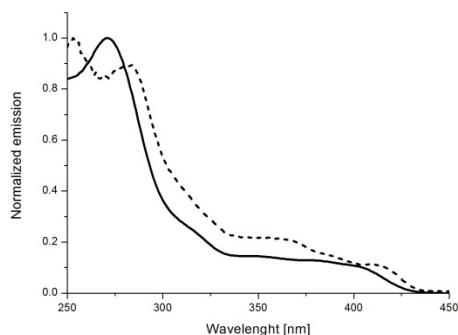


Figure S2. Excitation spectra of complex [10] at rt (solid line) and 77 K (dashed line).

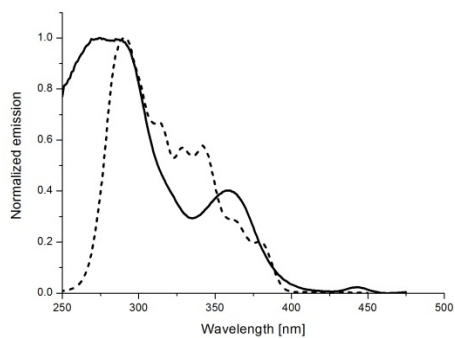


Figure S3. Excitation spectra of complex [11] at rt (solid line) and 77 K (dashed line).

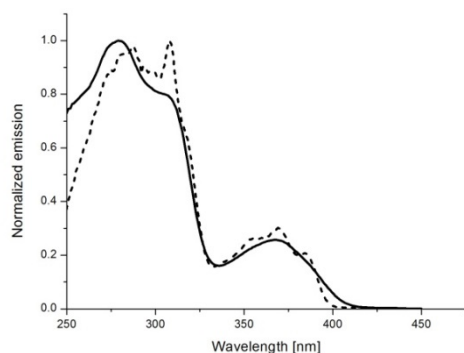


Figure S4. Excitation spectra of complex [13] at rt (solid line) and 77 K (dashed line).

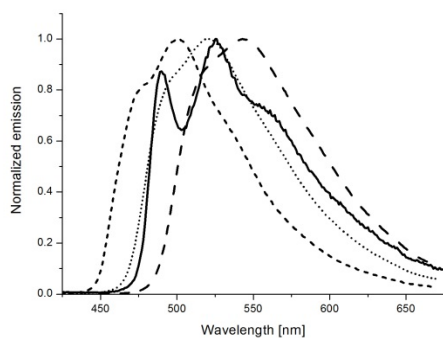


Figure S5. Emission spectra of [9] (solid line), [10] (long dashed line), [11] (dotted line) and [13] (short dashed) in neat films. Excitation wavelengths: 357 nm, 354 nm, 336 nm and 308 nm, respectively.

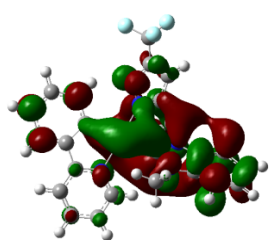
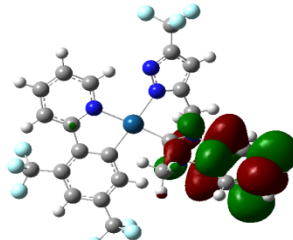
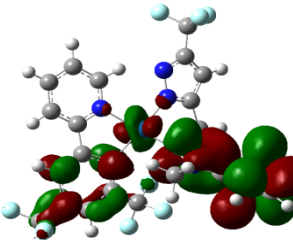
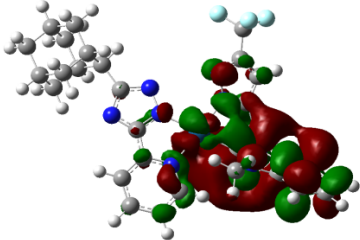
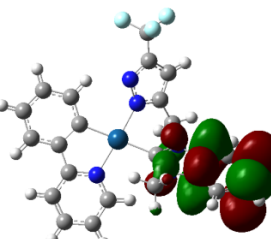
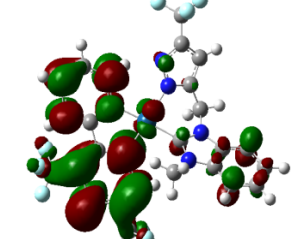
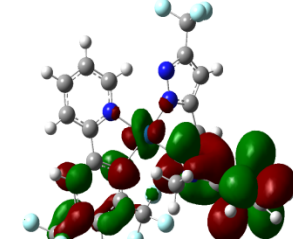
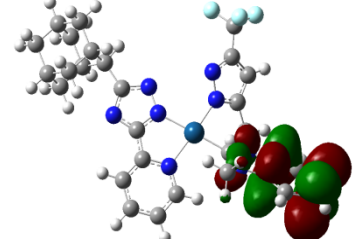
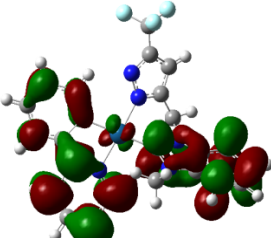
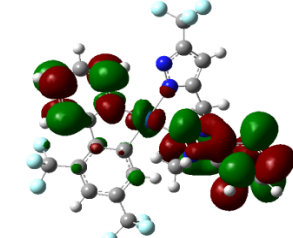
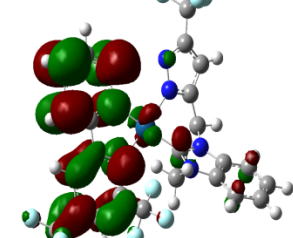
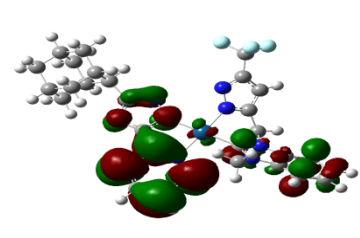
Computational results

Table S1. List of selected molecular orbital energies [eV] for the investigated complexes, and HOMO–LUMO gaps.

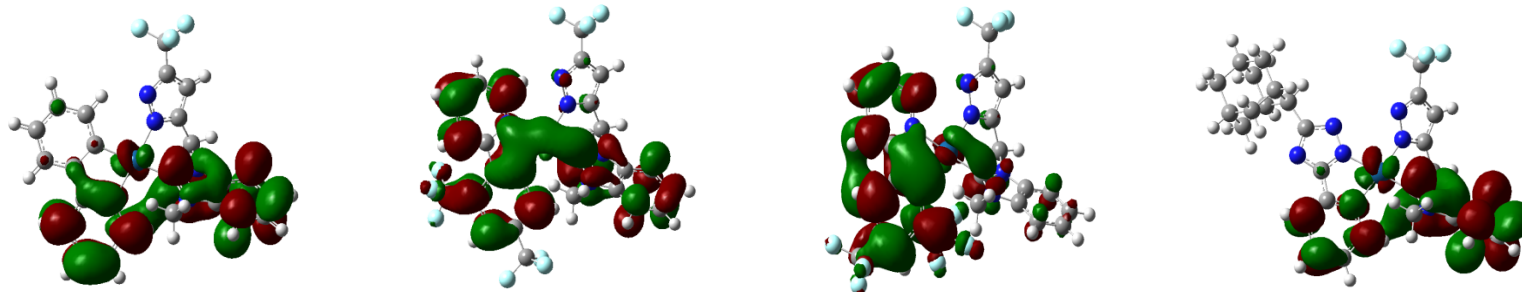
orbital	[9]	[10]	[11]	[13]
LUMO + 4	-0.194	-0.557	-0.360	-0.295
LUMO + 3	-0.409	-1.138	-0.392	-0.401
LUMO + 2	-1.297	-1.428	-1.267	-1.135
LUMO + 1	-1.357	-1.790	-1.938	-1.337
LUMO	-1.982	-2.705	-2.452	-2.057
HOMO	-6.075	-6.735	-6.751	-6.327

HOMO - 1	-6.349	-7.160	-7.109	-6.987
HOMO - 2	-6.537	-7.211	-7.156	-7.155
HOMO - 3	-6.684	-7.318	-7.257	-7.178
HOMO - 4	-6.814	-7.636	-7.480	-7.200
HOMO - 5	-7.241	-7.713	-7.630	-7.294
<hr/>				
HOMO-LUMO gap	4.093	4.030	4.299	4.270
<hr/>				

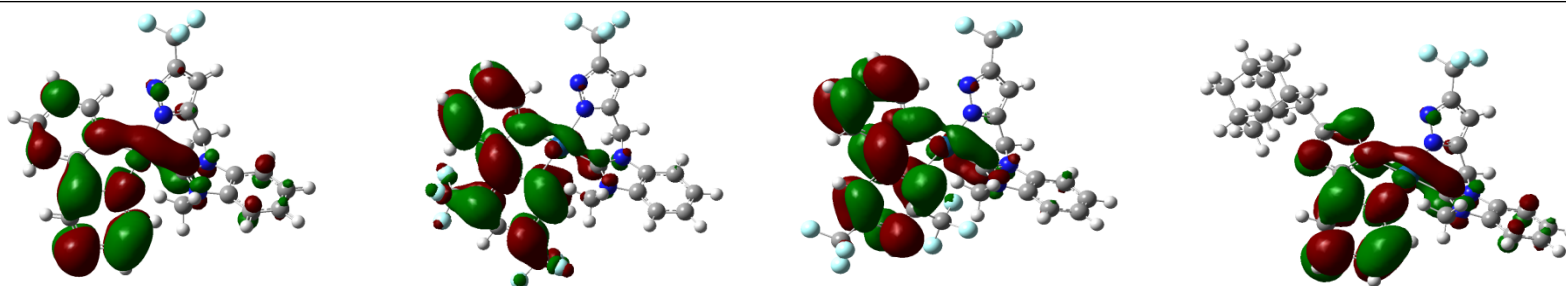
Table S2. Isodensity surfaces plots of selected orbitals for the complexes [8], [9], [10] and [11] in the gas phase at their optimized ground-state geometry. Isodensity value $0.02 e \text{ Bohr}^{-3}$.

Orbitals	[9]	[10]	[11]	[13]
LUMO + 4				
LUMO + 3				
LUMO + 2				

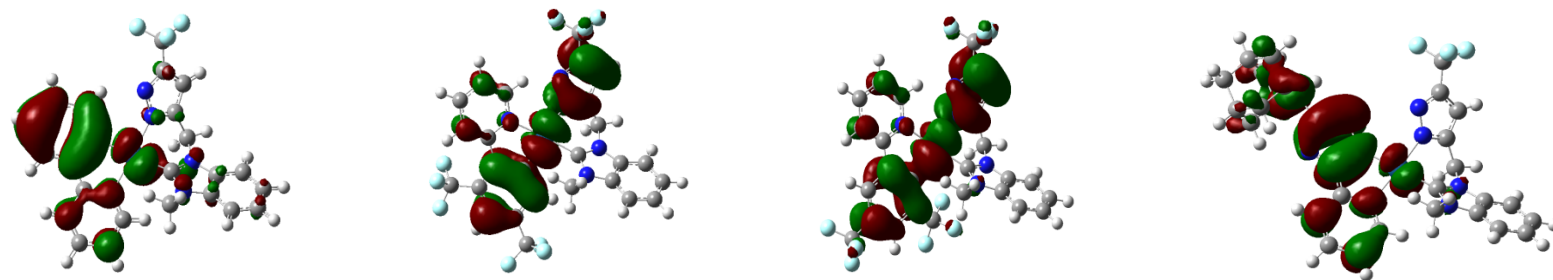
LUMO + 1



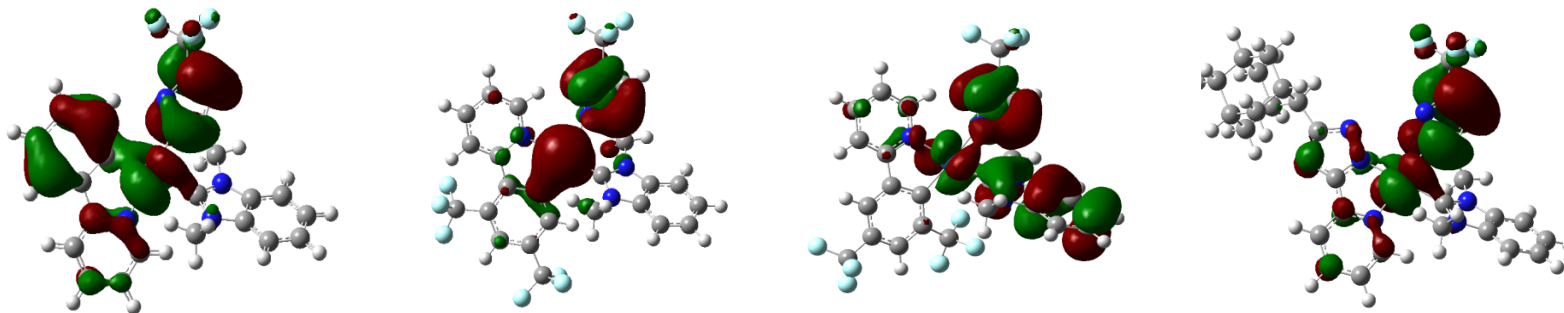
LUMO



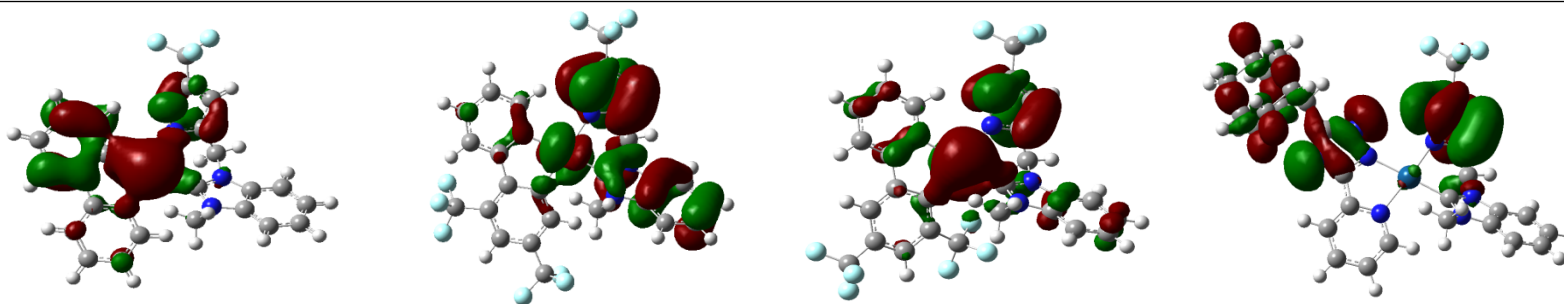
HOMO



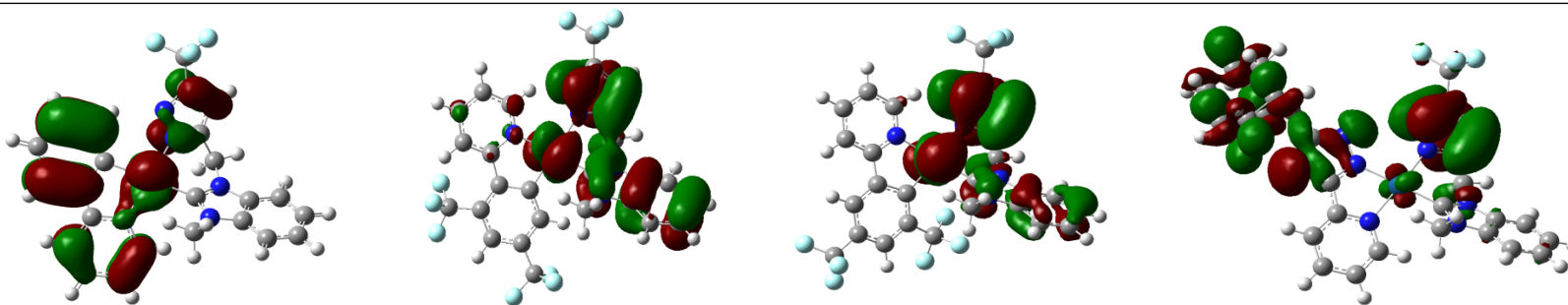
HOMO - 1



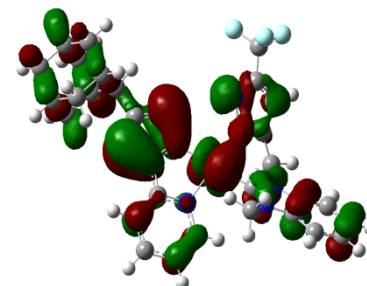
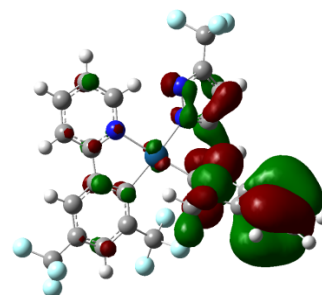
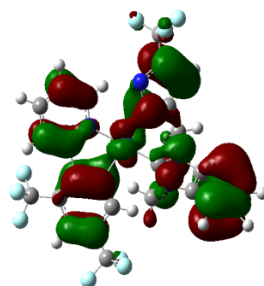
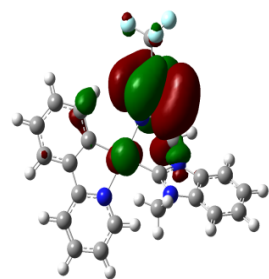
HOMO - 2



HOMO - 3



HOMO - 4



HOMO - 5

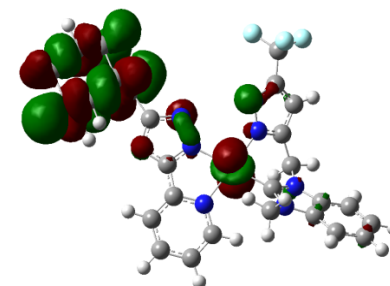
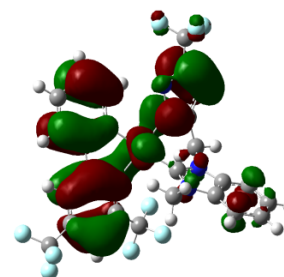
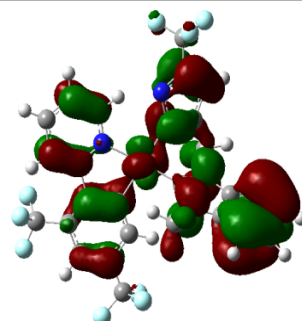
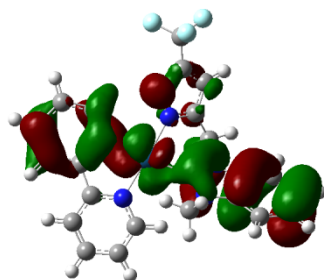


Table S3. Computed excitations energies and oscillator strengths for the complexes [9], [10], [11] and [13]. Except for S_i and T_i, only calculated excitations with $f \geq 0.05$ are listed. Also, only singly excited configurations contributing more than 20% are reported, together with the corresponding transition energy and expansion coefficient.

[9]	[10]	[11]	[13]
488, 2.5423 (0.000) (³ A) (0.57) HOMO → LUMO	480, 2.5847 (0.000) (³ A) (0.55) HOMO → LUMO	456, 2.7138 (0.000) (³ A) (0.47) HOMO → LUMO	448, 2.7634 (0.000) (³ A) (0.39) HOMO → LUMO
399, 3.1084 (0.008) (¹ A) (0.70) HOMO → LUMO	394, 3.1504 (0.0452) (¹ A) (0.69) HOMO → LUMO	368, 3.3678 (0.0439) (¹ A) (0.69) HOMO → LUMO	370, 3.3526 (0.0411) (¹ A) (0.70) HOMO → LUMO
346, 3.5881 (0.1405) (¹ A) (0.57) HOMO-1 → LUMO (¹ A) (0.35) HOMO-2 → LUMO (¹ A) (0.15) HOMO-3 → LUMO	331, 3.7483 (0.0881) (¹ A) (0.54) HOMO-2 → LUMO (¹ A) (0.41) HOMO-3 → LUMO	320, 3.8716 (0.1159) (¹ A) (0.62) HOMO-1 → LUMO (¹ A) (0.17) HOMO → LUMO+1	299, 4.1526 (0.1371) (¹ A) (0.63) HOMO-1 → LUMO (¹ A) (0.18) HOMO-4 → LUMO (¹ A) (0.16) HOMO-2 → LUMO
325, 3.8187 (0.0455) (¹ A) (0.41) HOMO → LUMO+1 (¹ A) (0.36) HOMO → LUMO+2	294, 4.2250 (0.1139) (¹ A) (0.54) HOMO-4 → LUMO (¹ A) (0.15) HOMO-6 → LUMO	313, 3.9605 (0.0913) (¹ A) (0.65) HOMO → LUMO+1	289, 4.2935 (0.0555) (¹ A) (0.43) HOMO → LUMO+2 (¹ A) (0.29) HOMO-4 → LUMO
313, 3.9642 (0.0827) (¹ A) (0.53) HOMO → LUMO+1	277, 4.4779 (0.0616) (¹ A) (0.53) HOMO-7 → LUMO (¹ A) (0.19) HOMO-6 → LUMO	283, 4.3859 (0.0557) (¹ A) (0.60) HOMO-1 → LUMO+1 (¹ A) (0.21) HOMO-3 → LUMO+1	280, 4.4277 (0.2214) (¹ A) (0.53) HOMO → LUMO+2 (¹ A) (0.28) HOMO-3 → LUMO (¹ A) (0.27) HOMO-2 → LUMO
307, 4.0397 (0.1090) (¹ A) (0.40) HOMO → LUMO+2 (¹ A) (0.15) HOMO-1 → LUMO	270, 4.6021 (0.0693) (¹ A) (0.45) HOMO-8 → LUMO (¹ A) (0.17) HOMO-7 → LUMO	280, 4.4222 (0.0875) (¹ A) (0.41) HOMO-4 → LUMO	276, 4.4951 (0.0539) (¹ A) (0.64) HOMO-5 → LUMO
280, 4.4306 (0.1474) (¹ A) (0.46) HOMO-5 → LUMO (¹ A) (0.23) HOMO-1 → LUMO+1	267, 4.6506 (0.1946) (¹ A) (0.45) HOMO-2 → LUMO+1 (¹ A) (0.23) HOMO-8 → LUMO (¹ A) (0.22) HOMO → LUMO+3	273, 4.5448 (0.0521) (¹ A) (0.32) HOMO-6 → LUMO (¹ A) (0.27) HOMO → LUMO+2	252, 4.9167 (0.0472) (¹ A) (0.62) HOMO-1 → LUMO+1 (¹ A) (0.11) HOMO → LUMO+1
273, 4.5298 (0.0651) (¹ A) (0.53) HOMO-3 → LUMO+1 (¹ A) (0.31) HOMO-3 → LUMO+2	261, 4.7607 (0.0786) (¹ A) (0.53) HOMO-3 → LUMO+1 (¹ A) (0.17) HOMO → LUMO+3	265, 4.6770 (0.1362) (¹ A) (0.51) HOMO → LUMO+3 (¹ A) (0.16) HOMO-1 → LUMO+3	251, 4.9420 (0.1138) (¹ A) (0.40) HOMO-3 → LUMO+1 (¹ A) (0.28) HOMO-2 → LUMO+1

	256, 4.8514 (0.2396) (1A) (0.53) HOMO → LUMO+3 (1A) (0.22) HOMO-9 → LUMO	262, 4.7421 (0.0495) (1A) (0.42) HOMO-2 → LUMO+2 (1A) (0.23) HOMO-3 → LUMO+2	
		254, 4.8900 (0.1566) (1A) (0.51) HOMO-1 → LUMO+3 (1A) (0.31) HOMO-4 → LUMO+1	

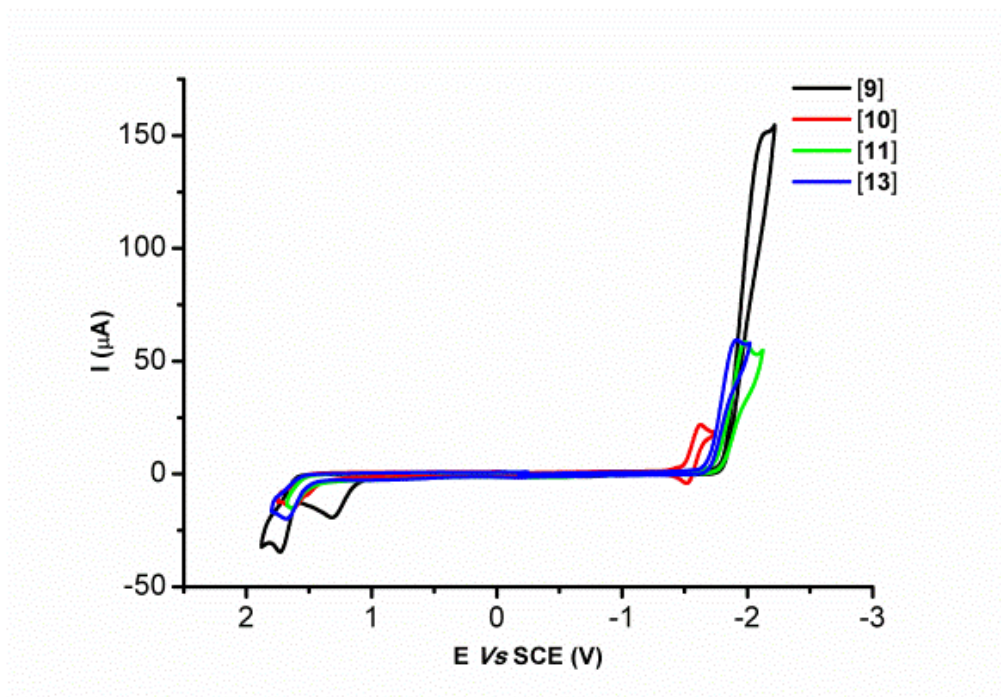
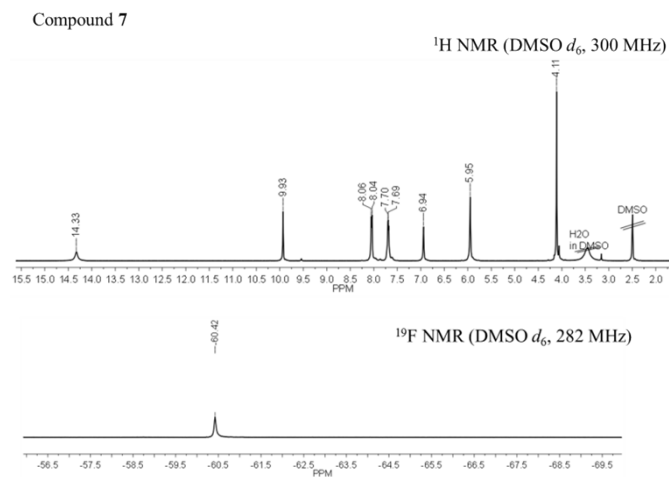


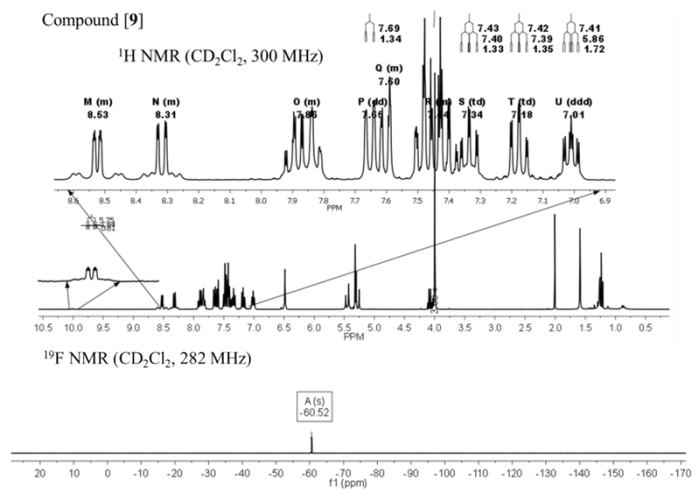
Figure S6. CV plots of complexes [9], [10], [11], [13].

Figure S7. NMR spectra of ligand precursor **7** and complexes **[9]**, **[10]**, **[11]**, **[13]**.

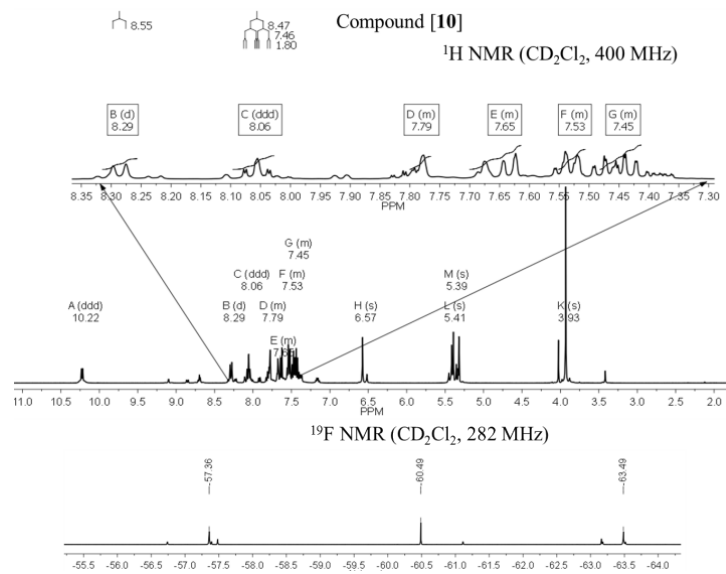
a. Compound **7** (ligand precursor)



b. Compound **[9]**

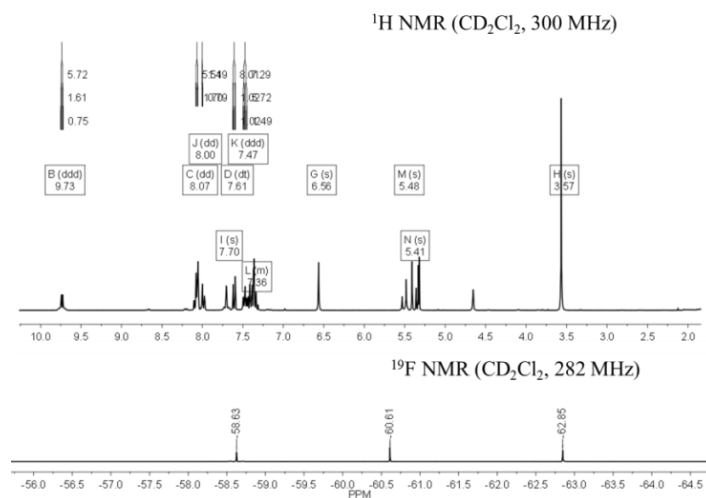


c. Compound [10]



d. Compound [11]

Compound [11]



e. Compound [13]

Compound [13]

